JOURNAL OF OPTOELECTRONICS AND ADVANCED MATERIALS, Vol. 11, No. 5, May 2009, p. 635 - 643

The influence of change in silane concentration and substrate temperature on optical properties of hydrogenated microcrystalline silicon films

R. I. BADRAN*, S. AL-HENITI, F. S. AL-HAZMI, A. A. AL-GHAMDI, J. LI[a], S. XIONG[a]
Physics Department, King Abdulaziz University, P.O. Box 80203, Jeddah, Saudi Arabia
[a]*Institute of Optoelectronics, Nankai University, Tianjin, 300071, China*

The influence of change in deposition conditions of silane concentration and substrate temperature on optical properties of hydrogenated microcrystalline silicon thin film samples prepared by Plasma Enhanced Chemical Vapor Deposition (PECVD) technique, are investigated. The crystalline volume fraction for the samples determined from Raman spectra are correlated with the silane concentration, substrate temperature, deposition rate, absorption coefficient, refractive index and optical energy gap. In addition, a decrease in crystalline volume fraction is found accompanied by a decrease in both dark and photo- conductivities. The values of optical parameters (refractive index and absorption coefficient) are calculated from the transmission spectra in the range 400-2500nm and then used to determine optical band energy gap and Urbach energy. All these values are fairly compared to those obtained by different techniques.

(Received April 20, 2009; accepted May 25, 2009)

Keywords: PECVD; a-Si: H and μc-Si:H; Electrical Conductivity; Optical Properties; Infrared and Raman Spectra

1. Introduction

Hydrogenated amorphous silicon (a-Si: H) and microcrystalline silicon (μc-Si: H) have widespread applications in solar cells and transistors in addition to several other electronic devices. Several techniques have been employed to prepare suitable thin films for such electronic devices. One of the widely used techniques is the radio frequency (rf) glow discharge decomposition of silane. In this technique it was found that several deposition parameters, such as gas flow rate, excitation power, pressure, substrate temperature and dilution of the source gas (silane) with other gases (argon, hydrogen, or helium) will influence the structure and properties of the growth of a-Si:H thin film [1, 2]. The effect of argon (Ar) dilution on the structure and optical properties of hydrogenated amorphous and microcrystalline films deposited by rf glow discharge decomposition of silane has been demonstrated [1]. The effect of hydrogen dilution on the optical properties of amorphous-microcystalline line mixed-phase Si: H films prepared by glow-discharge decomposition of mixed SiH_4-H_2 gas was also studied [2, 3]. A detailed experimental study on the effect of hydrogen dilution in terms of the deposition rate, the optical band gap, the Urbach energy, the defect density of states, the hydrogen content and the refractive index has been discussed [2]. The Plasma Enhanced Chemical Vapor Deposition (PECVD) has also become a prominent technique in preparing quality thin films that are used in large-area devices, such as photovoltaic (PV) cells and thin-film transistors (TFT) [4, 5]. The most common available technique that enables us to study the optical properties of thin films is optical transmission spectroscopy. The optical transmission spectroscopy, which is an easy and a nondestructive technique, provides information about several optical parameters like refractive index n (λ), extinction coefficient k (λ), absorption coefficient $\alpha(\lambda)$, film thickness and optical energy gap. Different methods have been employed in the analysis of optical transmission data obtained from spectrophotometery [6-12]. The simplest commonly used method is that of Swanepoel [10-11].

In this study, optical properties of two sets of μc-Si: H thin film samples prepared by PECVD technique using H_2-diluted SiH_4 gases, at different silane concentrations (SC= SiH_4/ (SiH_4 + H_2)) and substrate temperatures T_s, were studied. This study of optical properties together with electrical properties is correlated to some structural aspects extracted from Raman spectra. One set of samples (set I) was prepared with different silane concentration (SC= 0.67, 2.0, 3.0 and 4.0 %) at standard conditions of 220°C substrate temperature, 25W power and 120 Pa pressure. The other set of samples (set II) was prepared with different substrate temperatures (T_s= 100, 150, 220 and 250°C) under the same conditions of power and pressure but with a silane concentration SC=2.0%. Raman measurements have been conducted on both sets of samples and the crystalline volume fraction for each sample was found. The transmission data for the two sets of samples obtained from optical measurements using JASCO double-beam spectrophotometer have been analyzed using the method of Swanepoel [10]. The effect of silane concentration and substrate temperature on the optical energy gap, absorption coefficient and refractive index has been discussed. The obtained values of

absorption coefficient, refractive index and energy gap are compared to those of others.

2. Experimental techniques

2.1 Sample preparation

Microcrystalline silicon samples have been prepared by Plasma Enhanced Chemical Vapor Deposition (PECVD) technique at different preparation conditions. A set of microcrystalline silicon samples (set I) with silane concentrations (SC) of 0.67, 1.0, 2.0, 3.0 and 4.0% , using H_2-diluted SiH_4 gases, was prepared at standard power and pressure of 25W and 120 Pa, respectively, when the substrate temperature was maintained at T_s= 220°C. Another set of microcrystalline silicon samples (set II) was also prepared using same type of substrates with a fixed silane concentration of SC=2% at same conditions of pressure and power, but at different substrate temperatures of T_s=100, 150, 220 and 250°C. All samples were deposited on 7059 Corning glass substrates.

2.2 Raman Measurements

The crystallinity of μc-Si: H was investigated by Raman spectra using 632.8nm He-Ne laser. The degree of crystallinity is estimated by finding the crystalline volume fraction X_c. Here, X_c is determined by using the well-known ratio $X_c= I_c/(I_c + I_a)$, where I_c and I_a are the crystalline and amorphous intensity peaks which are extracted from the Raman scattering spectra. The values of X_c for both sets of samples are listed in tables 1 and 2.

2.3 Optical and Electrical Measurements

Optical measurements were conducted using JASCO V-570, UV-VIS-NIR double beam spectrophotometer. Transmission spectra were recorded in the range of wavelengths 400-2500 nm. Spectrophotometric measurements for all samples were performed at room temperature.

Steady state photocarrier grating set-up was used to measure the dark and photo- conductivities. Coplanar Al contacts were used for these electrical measurements. All measurements were conducted at room temperature.

3. Determination of optical constants

A FORTRAN program has been developed to calculate the values of n (λ), k (λ) and to estimate the values of thickness for the μc-Si: H samples using the appropriate formulas (equations A1, A3, 4, 5, 9, 17-20, 22 and 27) of Ref [10]. Corrections for the initial calculated values of n (λ) and thickness have also been performed. The values of thickness are determined using the suggested graphical method through employing the relation

$$\frac{\ell}{2} = 2d(n(\lambda)) - m, \tag{1}$$

where ℓ = 0, 1, 2, 3…etc. The initial values of n obtained from above-mentioned equations are used. Only the values of λ and n of the extrema are used to determine the number m and the sample thickness, d. The program makes its iteration to search for the nearest integer (or half integer if the first extreme is a minimum) which gives the best straight line fit. The value of the thickness is obtained from the slope of the straight line. Accurate values of n (λ) can be reached by using the obtained accurate values of m and d, and using the relation

$$2\,n(\lambda)\,d = m\lambda. \tag{2}$$

The relation used to fit the obtained values of n (λ) is:

$$n(\lambda) = \frac{A}{\lambda^2} + B, \tag{3}$$

where A and B are fitting parameters.

The optical energy gap for the samples, E_g, can be determined from variation of $(\alpha h\nu)^{0.5}$ against photon energy, $h\nu$, using the well-known Tauc relation

$$(\alpha h\nu) = C(h\nu - E_g)^2, \tag{4}$$

where C is the edge width parameter, which is related to the width of the band tails or disorder in the sample.

4. Results and analysis

Fig. 1 shows Raman spectra for μc-Si: H thin films (set I) prepared at different silane concentrations (SC). The prominent peaks around 516 $cm^{-1}$are indication for the presence of microcrystallites in the silicon material. The shift in the peaks asserts the change in the degree of crystallinity with the change in silane concentration. Here, the increase in the deposition rate of the film may have its effect on changing the spectrum shift in the Raman spectra from 516.73 to 519.8 cm^{-1}. The substrate temperature has also an effect on changing the position of Raman peaks for set II. The peaks are shifted towards lesser wavelengths when the temperature decreases from T_s =250°C to 100°C, as shown in Fig. 2.

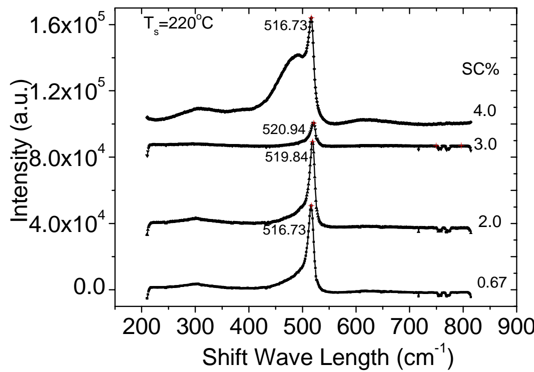

Fig. 1. Raman Spectra of μc -Si: H samples prepared using PECVD technique with different silane concentrations (set I) at substrate temperature, excited power and pressure of 220 °C, 25 W and 120 Pa, respectively.

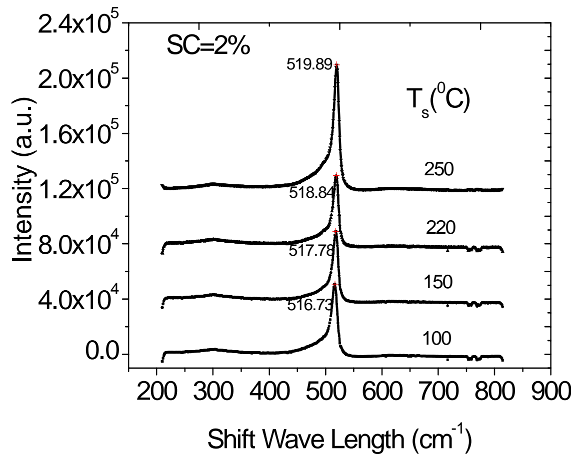

Fig. 2. Raman Spectra of μc -Si: H samples prepared using PECVD technique with different substrate temperatures (set II). The silane concentration, excited power and pressure are kept at 2%, 25W and 120Pa, respectively.

Both the dark conductivity σ_d and the photocondcutivity σ_{ph} of the samples increase with the decrease in SC and the increase in substrate temperature, as shown in tables 1 and 2. The values of photoconductivity σ_{ph} are correlated with the values of σ_d for set I, as shown in table 1. Similar correlation for both σ_d and σ_{ph} with the increase in the substrate temperature (set II), is shown in table 2. The low value of σ_d, although the crystalline volume fraction is high, indicates that a high value of defect density does exist in the sample under study [13]. The decrease in dark conductivity σ_d may be attributed to the shift of Fermi level towards midgap. Therefore, such change in conductivities is influenced by the position of the Fermi level in the upper half of the band gap which determines the occupation of defects levels and electron capture and recombination times. Moreover, the clear tendency of increase in dark conductivity with increasing T_s can be noted to be in good agreement with the Raman spectra in figure 2. Our results are in agreement with those obtained by others [14].

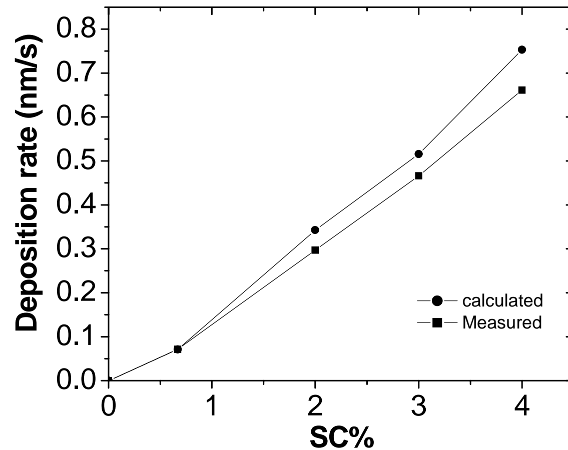

Fig. 3. Plot of deposition rate as a function of silane concentration. Calculated values of deposition rate are compared to experimental values. The values of thickness were calculated using the method of Swanepoel [10]. Film thickness was measured by AMBIOS Tech. Inc. Profilometer

The variation of deposition rate against silane concentration, at a fixed substrate temperature T_s is shown in figure 3, where both experimental data and theoretical results of deposition rate are compared. When the substrate temperature T_s is changed from 100 to 250^{0}C, at SC=2%, the deposition rate is almost 0.31±0.07 nm/s. However, the calculated deposition rate is found 0.42±0.035 nm/s. The theory of Swanepoel [10] is used to estimate the film thickness values and then to determine the values of deposition rate.

Table 1. The crystalline volume fraction X_c, Urbach energy E_u, dark conductivity σ_d and photoconductivity σ_{ph} for μc -Si: H samples prepared at different silane concentrations, with standard temperature, power and pressure of 220°C, 25W and 120Pa, respectively.

μc-Si:H Sample	X_c (%)	SC (%)	σ_d (Ω^{-1} cm^{-1})	σ_{ph} (Ω^{-1} cm^{-1})	E_u (meV)	A ×10^5 (nm)^2	B
A	75.1	0.67	1.98E-3	6.83E-4	98.7	2.075	3.10
B	73.1	2.0	1.37E-3	8.30E-4	446.7	1.480	2.90
C	55.0	3.0	5.12E-5	3.16E-4	138	2.256	3.08
D	36.9	4.0	1.66E-6	6.21E-5	290	2.158	3.12

Table 2. The crystalline volume fraction X_c, Urbach energy E_u, dark conductivity σ_d and photoconductivity σ_{ph} for μc -Si: H samples prepared at different substrate temperatures with fixed silane concentration, power and pressure of 2%, 25W and 120Pa, respectively. The experimental deposition rate is almost 0.31±0.07 nm/s. The estimated deposition rate is 0.422±0.035 nm/s which is calculated using the method of Swanepoel [10].

μc-Si:H Sample	X_c (%)	T_s (°C)	σ_d ($\Omega^{-1}cm^{-1}$)	σ_{ph} ($\Omega^{-1}cm^{-1}$)	E_u (meV)	A $\times10^5$ $(nm)^2$	B
E	69.8	100	4.86E-7	9.73E-6	159	1.497	3.03
F	79.6	150	2.01E-6	8.75E-6	175	1.782	3.02
G	82.8	220	9.17E-4	5.76E-4	582	3.953	2.84
H	77.4	250	1.63E-3	7.47E-4	166	1.934	3.11

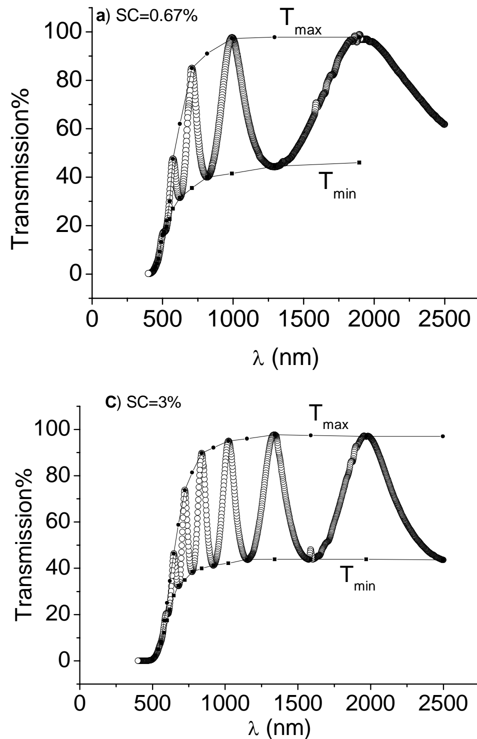

Fig. 4. Transmission spectra of μc -Si: H samples (set I) prepared using PECVD technique with (a) SC= 0.67%, (b) SC= 2%, (c) SC= 3% and (d) SC= 4% at substrate temperature, excited power and pressure of 220°C, 25W and 120Pa, respectively. Optical measurements were conducted using JASCO double beam spectrophotometer. T_{max} and T_{min} (lines + symbols) were obtained from the extrema of experimental data of transmission (symbols) [10].

For set I, the maximum and minimum transmission values were extracted and plotted together with the transmission data in figure 4. The transmission data for set II, where the films were prepared at different substrate temperatures T_s, were shown in figure 5. Similar procedure was followed for analysis of data for set II, but the extracted maxima and maxima are not shown here. All the films, for both sets, have exhibited good transparency in the infrared region and this transparency is degraded in the visible region. The spectra show interference pattern with sharp fall off in the transmittance at the band edge, which is an indication of good crystallinity.

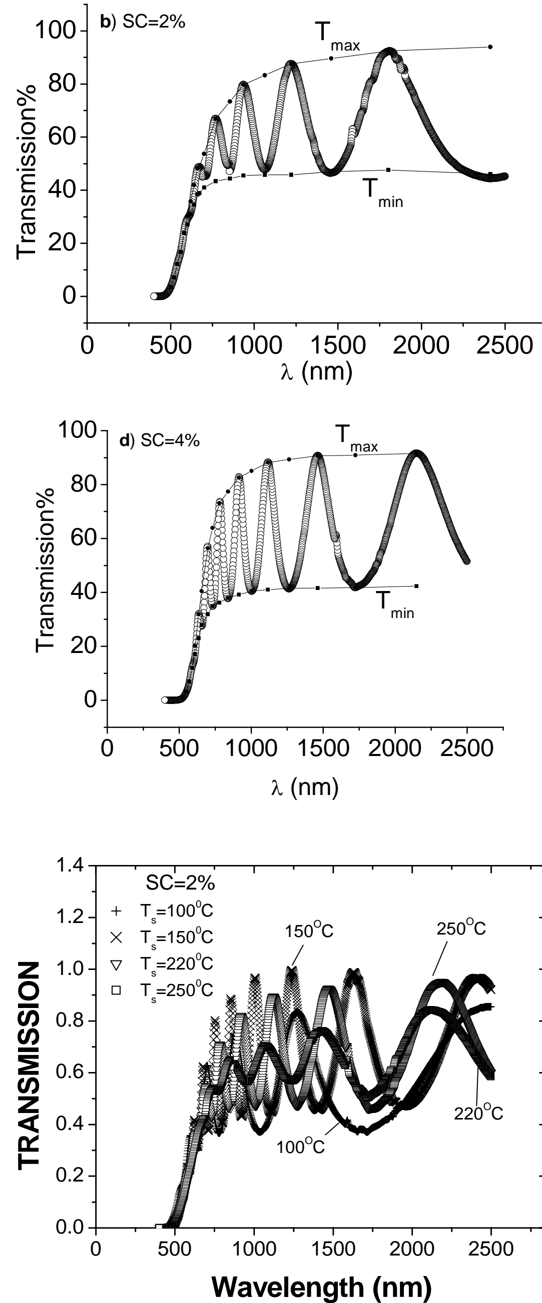

Fig. 5. Transmission spectra of μc -Si: H samples (set II) prepared using PECVD technique with different substrate temperatures at SC= 2%.

The best-obtained fitting parameters, *A* and *B*, for both sets are listed in tables 1 and 2. Both calculated and best-fitted values of *n* (λ) are plotted against wavelength and shown in figure 6 for all samples (A-D) of set I. In this figure, the error bars indicate the uncertainty in calculated values of *n* (λ). The error in refractive index is determined to be about 1% of the corrected value. Both best-fitted and calculated dispersion curves of refractive index of μc-Si: H samples at different silane concentrations are compared to the dispersion curve of crystalline silicon (c-Si) sample. It is interesting to note that most of the μc-Si: H samples have dispersion curves close to but relatively lower than the c-Si dispersion curve. It is also noted that the fitting relation can produce each required transmission spectrum with a reasonable accuracy. Therefore, the values of α (λ) have been determined using the relevant formulas [10] and the obtained fitted values of *n* (λ). It must be noted that the five formulae of Ref. 10, are employed to determine the value of α (λ). The average value and the corresponding uncertainty at each wavelength are considered and used in the present analysis.

The variation of absorption coefficient against hν for both sets is shown in figure 7. In figure 7-a the absorption spectrum of a c-Si sample is compared to the absorption spectra of μc -Si: H samples where the samples with high crystallinity have absorption coefficients close to those of c-Si while those with lower crystallinity show higher absorption, at photon energies larger than 1.7eV. This behaviour may be attributed to the small volume fraction of amorphous tissue in the μc-Si: H samples with high crystallinity [5, 14]. Here, larger number of carriers may be generated in the amorphous tissue than in the crystallites. However, at smaller energies (< 1.7eV) the trend of absorption does not clearly increase with increasing crystallinity where free carriers are responsible for absorption.

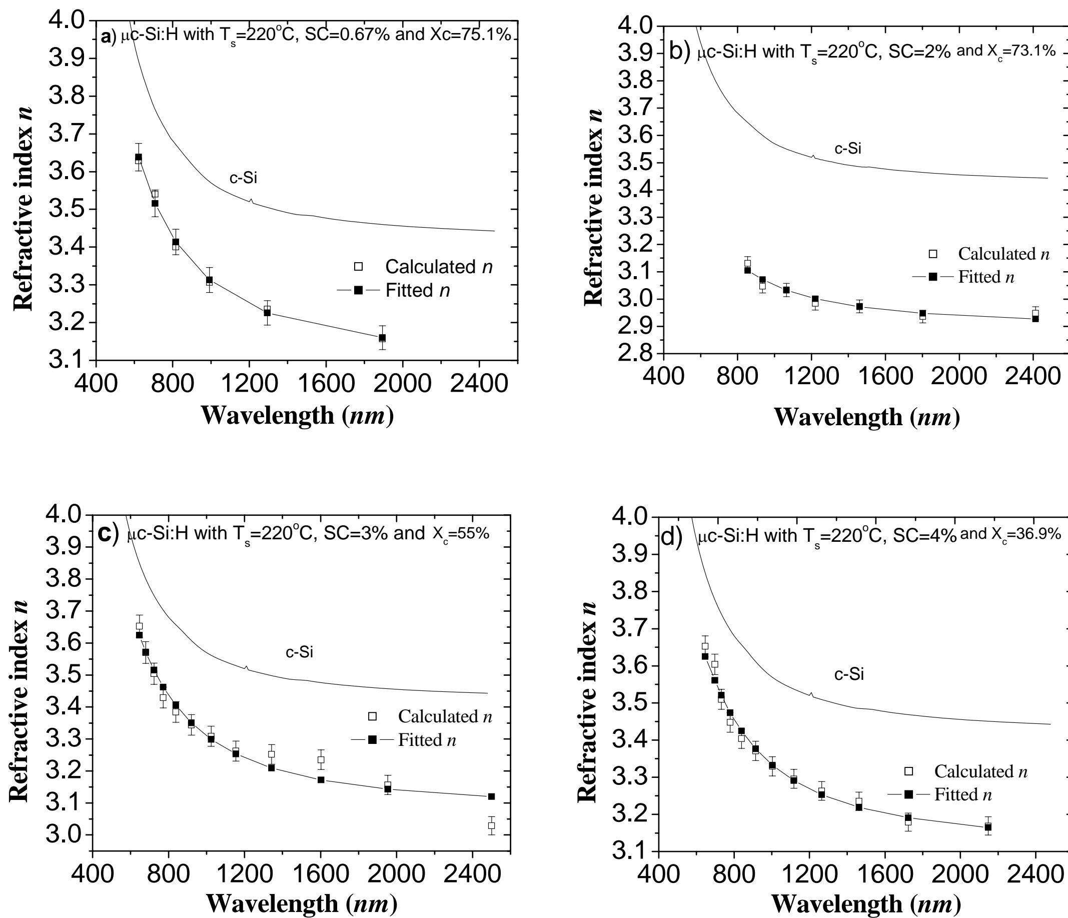

Fig. 6. Variation of refractive index, n, versus photon energy for μc -Si: H samples (set I) with different silane concentrations of a) SC=0.67%, b) SC= 2%, c) SC= 3% and d) SC= 4% at substrate temperature, power and pressure of 220^{0}C, 25W and 120Pa, respectively. The dispersion curve of refractive index of c-Si sample is also shown.

The behaviour of the variation in absorption coefficient is mild for set II, when the substrate temperature is changed from 100 to 250°C (samples E-H), as shown in figure 7-b. Here, the trend of the change in absorption due to the increase in X_c of samples is as expected at both regions of smaller than and larger than

photon energy of 1.7eV except that of sample G. This is consistent with the relative change in crystallinity among samples of set II as compared to that among samples of set I, where samples G and B are excluded from both sets.

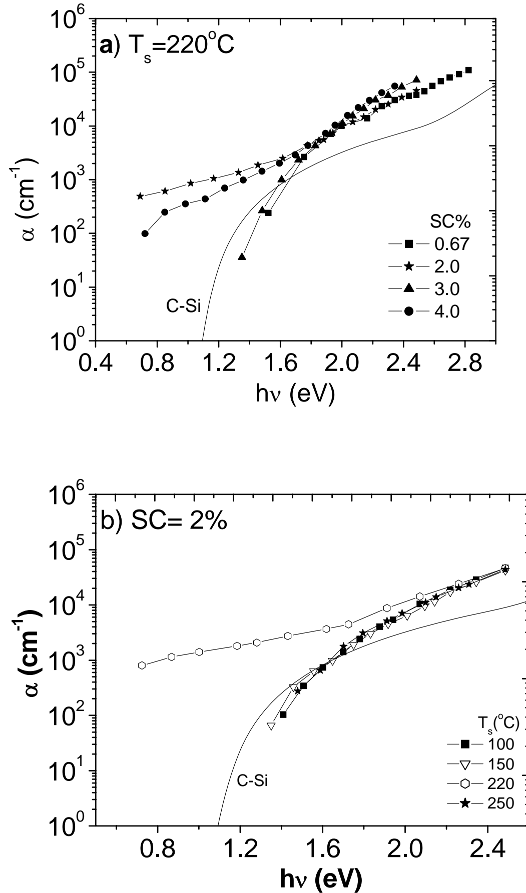

Fig. 7. Variation of absorption coefficient with photon energy for μc -Si: H samples at a) substrate temperature T_s=220^{0}C with different silane concentrations (set I), b) SC=2% with different substrate temperatures (set II). The absorption spectrum of a typical c-Si sample is compared to our absorption spectra of μc -Si: H samples.

It must be noted that the results of absorption coefficient at the low energy region have larger percentage of error than that at the other region. The reason for such discrepancies is due to some scattering points in one set of the data and low number of points available in the low range of absorption coefficient (2× 10^2 cm^{-1}> α > 5× 10^3 cm^{-1}) in another. Thus, this anomalous behaviour at low energies may be attributed to weak approximations made in the method at low absorption region. However, the global trend of change in absorption coefficient over the whole range of photon energies is discernible.

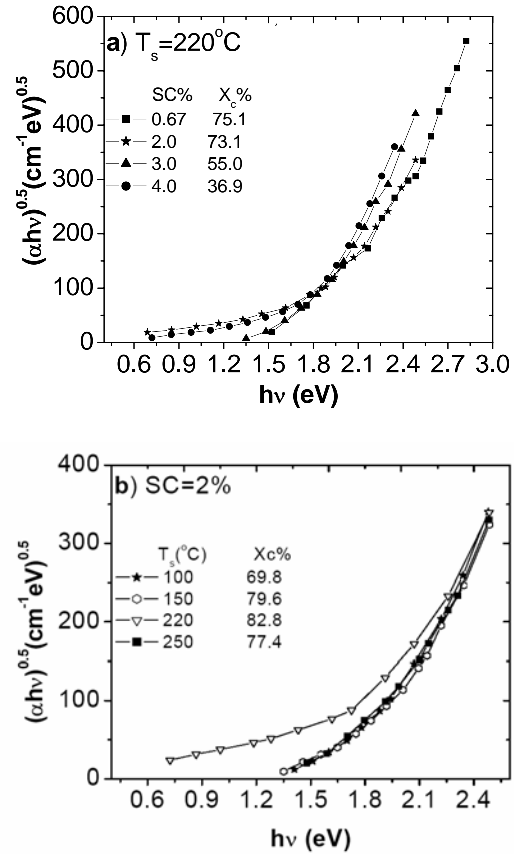

Fig. 8. Plot of $(\alpha h\nu)^{0.5}$ versus photon energy (a) for different silane concentrations of μc -Si: H films prepared at T_s=220°C (set I), (b) for different substrate temperatures of μc -Si: H films prepared at SC=2% (set II).

The sample prepared at SC= 2% and 220°C is shown to behave differently in both sets. It was thought that this sample has been contaminated with oxygen where the oxygen atoms act as O^+ donors in the Si-Si network of the sample [15]. However the sample (sample G) with X_c=82.8% of set II differs a little bit in its microstructure from that of sample B with X_c=73.1% of set I prepared at same deposition parameters. This may be attributed to the deposition system instability. In addition, the preparation of sample G was carried out in a different period from that of sample B where the deposition system has been shut down due to gas leakage check [15]. All this may give an explanation to the odd behaviour of this sample in both regions of smaller than and greater than 1.7eV photon energy of absorption spectrum. Moreover, there is a very small variance in the microstructure of these two samples. It was shown that the change in thickness also affects the film structure [15]. In general, the trend that has been exhibited for enhanced absorption in the near infrared and visible regions might make these samples good candidates for PV applications.

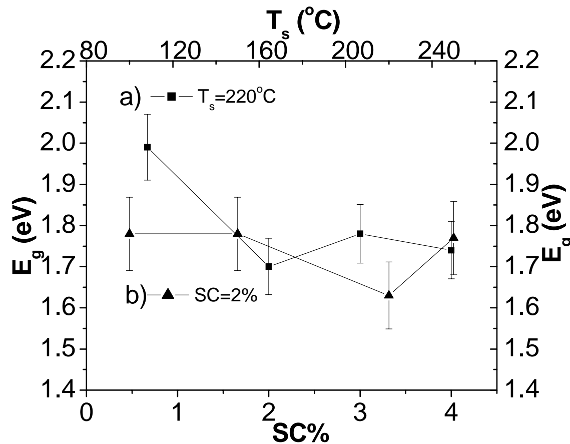

Fig. 9. a) Energy gap as a function of silane concentration for μc -Si: H films (set I) prepared at T_s=220^{0}C. b) Energy gap as a function of substrate temperature for μc -Si: H films (set I I) prepared at SC=2%.

The variation of $(\alpha h\nu)^{0.5}$ against photon energy for sets I and II is illustrated in figure 8. In figure 8-a, it is evident that the increase in the values of X_c leads to a decrease in values of $(\alpha h\nu)^{0.5}$, at photon energies greater than 1.7eV. For SC=2%, the decrease in substrate temperature leads to monotonic change in the values of $(\alpha h\nu)^{0.5}$ at photon energies greater than 1.7eV, as shown in figure 8-b. The optical energy gap is obtained from slope of the best straight line fit to the portion of the curve that corresponds to absorption coefficient greater than 5×10^3 cm^{-1} of figure 8. Different combination of points are taken to calculate the energy gap, when $\alpha > 5\times 10^3$ cm^{-1}, from the slope of different lines. Therefore, the average value of E_g is also obtained within an uncertainty. The plot of the variation in the energy gap with SC is shown in figure 9. The energy gap (E_g=1.74eV) at SC= 4% has a lesser energy than that (E_g=1.99eV) at SC= 0.67%. The error bars, shown in figure 9, show the uncertainty in the calculated energy gap which is estimated 4% of the average value of E_g. However, the decrease in energy gap as silane concentration changes from SC= 3% to 2% is an indication that not only the amount of the hydrogen content which plays a role in reducing the disorder, but also the way that such hydrogen is incorporated into the entire network of the material. Such trend in the change of the optical energy gap is found similar to that found by others [2, 5].

The energy gap decreases monotonically from E_g=1.78 to 1.77eV, at SC=2%, when the substrate temperature increases from 100 to 250^{0}C. The lowest value of E_g=1.63eV is for the sample prepared at 220°C (i.e. sample G). The energy gap against substrate temperature is also drawn in Fig. 9. Same as before, the average value of E_g is obtained and the uncertainty is about 5% of this value.

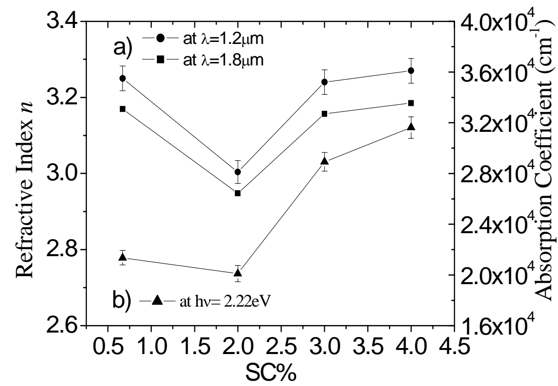

Fig. 10. a) Refractive index (at 1.2μm and 1.8μm) as a function of silane concentration for μc-Si: H films prepared at T=220^{0}C. b) Absorption coefficient (at energy 2.22eV) as a function of silane concentration for μc-Si: H films prepared at T=220^{0}C.

Although the trend of decrease in energy gap with increasing substrate temperature is found similar to that by other groups, but with a shallower fall off. This may indicate that the samples prepared with higher substrate temperatures exhibit an increase tendency of disorder. This trend for the energy gap is similar to that available in literature for microcrystalline semiconductors [2, 5].

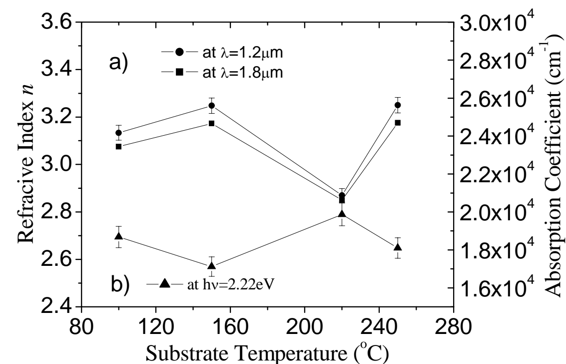

Fig. 11. a) Refractive index (at 1.2μm and 1.8μm) as a function of substrate temperature for μc-Si: H films prepared at SC= 2%. b) Absorption coefficient (at energy 2.22eV) as a function of substrate temperature for μc-Si: H films prepared at SC= 2%.

The analyses are conducted to find n in the non-absorbing region around 1.8μm and then extended to 1.2μm. The values of refractive index n at the non-absorbing region (λ=1.8μm) changes from 3.18 to 2.95 as SC changes from 4% to 2% and starts to increase to 3.17 at SC=0.67%, as shown in figure 10. By approaching towards the absorbing region (λ=1.2μm), the values of n changes from 3.27 to 3.0 as SC changes from 4% to 2%

and then increases to 3.25 at SC=0.67%, but retaining similar behaviour to that at λ=1.8μm. The beginning of fall off, shown in figure 10, with decreasing SC is consistent with that predicted by others [2] for SC < 3%. The error in calculated refractive index of 1% is shown to be as error bars in this figure. The absorption coefficient against photon energy, for set I, is also shown in the same figure. In this figure, α (hν) decreases from 3.16×10^4 cm^{-1} at SC=4% to 2.13×10^4 at SC=0.67% around the photon energy of 2.22eV. The fluctuation in α is determined to be approximately 7% of the calculated value and is indicated as error bars in figure 10. The change in crystalline volume fraction from 75.1 to 55 and to 36.9% of samples A, C and D, respectively, (apart from sample B) may reflect the type of behaviour in absorption coefficient at the region of larger photon energies.

Figure 11 shows the behaviour of refractive index for set II, when the substrate temperature (T_s) changes from 100 to 250°C, at the two different regions (λ=1.8μm and λ=1.2μm) as before. Similar behavior for *n* was found in the two regions. Here, *n* decreases (at λ=1.8μm) from 3.18 to 3.08 as T_s decreases from 250 to 100 ^{o}C, as shown in figure 11. However, its value at T_s=220°C is less than that at 100°C. The corresponding values of *n* at λ=1.2μm change from 3.25 to 3.14 when T_s decreases from 250 to 100 ^{o}C. The value of *n* at 220°C is 2.85. Again the error of 1% in the calculated refractive index is represented by the error bars in figure 11. The absorption coefficient exhibits a change from $1.81 \times 10^4 cm^{-1}$ to 1.98×10^4 cm^{-1} when T_s decreases from 250 to 220°C, and then decreases to 1.71×10^4 cm^{-1} when T_s is lowered to 150°C and then increases to $1.87 \times 10^4 cm^{-1}$ at 100°C. This monotonic behavior in absorption coefficient together with error bars which reflect the uncertainty of 4% in the calculated α, are shown in figure 11. This has a similar trend to that found by others [2]. We believe here that the dependence of the optical gap on the substrate temperature can be attributed to the hydrogen content in μc-Si: H samples. Since the relative change in crystallinity is small, this may indicate that relative change in grain sizes and grain boundaries is also small and this may result in monotonic behaviour in absorption coefficient.

The Urbach energy, E_u, is found to be in the range of 99-290meV, as seen in table 1, for the samples prepared at SC between 0.67 and 4% except that of 2% (sample B) which has very much higher Urbach energy (~ 447meV). The uncertainty in calculating E_u is about 18% of the average value. The samples prepared at substrate temperatures of 100, 150 and 250°C have Urbach energies of 160, 175 and 166meV, respectively, while the Urbach energy for the sample (sample G) prepared at T_s=220°C and SC=2% is about 582meV, as listed in table 2. Here, the fluctuation in calculating E_u is almost 13% of the average value. This indicates, again, that the samples B and G contain very much higher density of states than the other samples in sets I and II, respectively. The exponential absorption tail, here, is in a range wider than that of (250-300meV) found by others [16]. In addition, this range is obviously higher than that (50-60meV) found for a-Si: H samples [2, 17, 18].

Most of the above results are consistent with the structural behaviour shown by Raman spectra. However, it was shown that the decrease in SC might lead to a loose structure of μc-Si: H, which has a lot of defects and disorder. Such increase in defects may allow for Oxygen contamination in the samples [15]. Here, Oxygen plays the role of a donor, which causes to increase in conductivities at low SC. The barrier of amorphous tissue between grain columns mainly limits charge transport parallel to the substrate. Consequently, the grain column boundaries in addition to the Oxygen contamination affect the ability of conduction for the μc-Si: H films [15]. In addition, the higher level of carriers generation, at low SC, that enhances the absorption at large energies can be understood. It was believed that the volume fraction of microcrystalline material increases with increasing microcrystallite size. It was also shown that the grain size increases with the increase in the film thickness [15].

It was shown that upon the increase of T_s, at a fixed silane concentration, the predominant hydrogen-bonding configuration in the film changes from the dihydride (SiH_2) group to the mono-hydride (SiH) group. In addition, more hydrogenation with strong Si-H bonds may cause to enlarge the band gap as is well known in a-Si: H [2, 15]. Some of our results show that the optical energy gap is not strongly dependent on the hydrogen content but rather on the way it is incorporated into the random network. So investigation on the bonded-hydrogen content is highly recommended in order to have a concrete explanation to the effectiveness of hydrogen in reducing defects and disorder. This is beyond the scope of this paper.

The effect of the change in excited power and pressure on absorption coefficient, refractive index and optical energy gap for microcrystalline silicon films prepared by PECVD was investigated. In this study, the Swanepoel method was tested on transmission data only and the values of optical constants were fairly compared to those of others [19].

5. Conclusions

The hydrogenated microcrystalline silicon samples prepared by PECVD under different deposition conditions have been investigated. The optical parameters have been obtained from the optical transmission data only with a reasonable accuracy. These results were found consistent with the structural behavior shown by Raman spectra and with those obtained by others. The increase in silane concentration is found correlated with the deposition rate. However, such increase in SC is accompanied by a decrease in crystalline volume fraction and a corresponding decrease in both dark and photo-conductivities. The energy gap is also correlated to both substrate temperature and silane concentration. The studied hydrogenated microcrystalline silicon samples may be good candidates for photovoltaic applications due

to their behavior in visible and near infrared region of electromagnetic spectrum.

Acknowledgements

The authors are grateful to Dr Rudi Bruggemann for providing the conductivity data.

References

[1] U. K. Das, P. Chaudhuri, S. T. Kshirsager, J. Appl. Phys. **80**, 5389 (1996).
[2] M. Yamaguchi, K. Morigaki, Phil. Mag. **B79**, 387 (1999).
[3] M. Yamaguchi and K. Morigaki, J. Phys. Soc. Japan, **62**, 2913 (1993).
[4] G. Ambrosone, U. Coscia, S. Lettieri, P. Maddalena, C. Minarini, Mat. Sci. Eng. **B101**, 236 (2003).
[5] Y. H. Wang, J. Lin, C. H. A. Huan, Mat. Sci. Eng. **B104**, 80 (2003).
[6] M. H. Brodsky, M. Cardons, J. J. Cuomo, Phy. Rev. B **16**, 3556, (1997).
[7] E.C. Freeman and W. Paul, Phys. Rev. B **18**, 4288 (1978).
[8] Alvin M. Goodman, Appl. Opt. **17**, 2779 (1978).
[9] J. I. Szczyrbowski and A. Czapla, Thin Solid Films **46**, 127 (1977).
[10] R. Swanepoel, J. Phys. E: Sci. Instrum. **16**, 1214 (1983).
[11] R. Swanepoel, J. Phys. E: Sci. Instrum. **17**, 896 (1984).
[12] W. Hu.Flourence, Y. M. Chan, D. P. Webb, Y. C. Chan, Y. W. Lam, J. Electron. Mater. **25**, 1837 (1996).
[13] R. Bruggemann, R. I. Badran, S. Xiong, J. Optoelectron. Adv. Mat. **9**, 348 (2007).
[14] M. Mars, M. Fathallah, E. Tresso, S. Ferrero, J. Non-Cryst. Solids, **299-302**, 133 (2002).
[15] J. Li, Y. Li, C. Wu, Z. Meng, S. Zhao, S. Xiong and Z. Lizhu, Proceedings of Asia Display, **1-2**, 1178 (2007).
[16] P. Mishra, K. P. Jain, Mat. Sci. Eng. **B95**, 202 (2002).
[17] Y. Kanemitsu, Phys. Rev. **B53**, 13515 (1996).
[18] K. Murayama, S. Miyazaki, M. Hirose, Jpn. J. Appl. Phys. **31**(part 2), L1358 (1992).
[19] R. I. Badran, F. S. Al-Hazmi, S. Al-Heniti, A. A. Al-Ghamdi, J. Li and S. Xiong, Vacuum **83**, 1023 (2009).

*Corresponding author: rbadran_i@yahoo.com ; rbadran@kau.edu.sa